X. Miao, "Observation of Microcracks Formed in HA-316L Composites", *Materials Letters*, 57[12] (2003), pp. 1848-1853.

Observation of microcracks formed in HA-316L composites

X. Miao*
School of Materials Engineering, Nanyang Technological University, Nanyang Avenue, Singapore 639798

Abstract

Hydroxyapatite-stainless steel 316L fiber composites were prepared using as-supplied, 900^{o}C calcined, and 15 vol% yttria stabilised zirconia added hydroxyapatite powders. The reinforcements were 20 vol% chopped 316L fibres of length 1 mm and diameter 55 μm. Both hot isostatic pressing and spark plasma sintering were used to densify the composites with the processing temperatures varying from 825 to 950 ^{o}C, pressures from 20 to 140 MPa, and time from 10 to 180 min. The obtained composites were subjected to microstructural analysis using a scanning electron microscope. It was found that microcracking took place invariably in the hydroxyapatite matrices but near and around the 316L fibres. Such patterns of microcracks resulted from the thermal residual stresses developed during the cooling from the high temperatures and the intrinsic low mechanical strengths of the hydroxyapatite ceramics. Such microcracks may play important roles in the mechanical behaviour of the HA-316L fibre composites.

Keywords: hydroxyapatite, fibre, composite, thermal stress, microcrack
*Corresponding author. Tel.: +65-7904260; fax: +65-7909081.
E-mail address: asxgmiao@ntu.edu.sg (X. Miao).

1. Introduction

Hydroxyapatite (HA) ceramics have been intensively studied for bone repair and replacement applications due to their biocompatibility and ability to bond to bone [1]. However, the mechanical properties of HA ceramics are poor compared to those of natural bone [2,3]. Thus, various HA based composites have been studied [4]. Zirconia second phase has been commonly used in the HA ceramics due to its ability to inhibit grain growth and provide tetragonal to monoclinic phase transformation toughening and strengthening mechanisms [5]. Ceramic fibres such as carbon fibres have also been tried as reinforcements, but only limited improvement in mechanical property has been achieved in the composite [6]. A high fracture toughness has been obtained in HA ceramics reinforced with FeCr alloy fibres due to a crack bridging mechanism [7]. This has encouraged the author to work on a similar system, i.e. HA-stainless steel 316L fibre composite. However, the HA-316L fibre composite system has proved to be a challenging one, as the composite can not be densified by sintering in air due to the oxidation of the fibres. Sintering in protective atmosphere is also not effective, as the network of 316L fibres prevents densification and high temperature sintering results in decomposition of HA phase. Thus, hot pressing, hot isostatic pressing, or spark plasma sintering [8,9] should be used to densify the HA-316L composites without the decomposition of HA phase. However, the author has noticed another problem in the composite system; microcracks have been observed in the HA matrices. The purpose of this paper is to report on the observation of the microcracks in the HA-316L fibre composites prepared under various conditions. This problem of microcracking needs to be addressed so that possible solutions could be found by other researchers.

2. Experimental

The starting materials were as-supplied HA powder (Raw HA, E. Merck, D-6100 Darmstadt, Germany), as-supplied HA powder subjected to calcination at 900 ^{o}C for 1 hour (Calcined HA), ZrO_2(3 mol% Y_2O_3) powder (Y-TZP, Tosoh Corporation, Tokyo, Japan), and chopped stainless steel 316L fibers (length: 1 mm; diameter: 50 μm). Different amounts of the powders and the fibres were mixed in ethanol with an agitator. The formed power-fibre pastes were then dried, gently crushed, packed and formed by cold isostatic pressing and uniaxial pressing respectively to form cylindrical and disk-like specimens. The cylindrical specimens were encapsulated in evacuated and sealed stainless steel cans. To easily remove the specimens from the stainless steel cans, graphite foils were placed between the specimens and the stainless steel cans. Boron nitride foils would be better than graphite foils but were not available at the time. The encapsulated specimens were then hot isostatically pressed (HIP) at different temperatures and times but same pressure of 140 MPa (Table 1). The heating rate and the cooling rate were both set at 10 ^{o}C/ min. On the other hand, the pressed disks were densified by spark plasma sintering (SPS) on an SPS-1050 system. In the SPS process, a high heating rate of 100 ^{o}C/min was produced from direct current through the powder compact and a temperature of 950 ^{o}C was obtained and held for 10 min. A pressure level of 20 MPa was maintained during the high temperature holding period. Following densification at 950 ^{o}C, the samples were cooled to the room temperature at a cooling rate of ~ 50 ^{o}C/ min. The densified specimens were then cut, ground, polished and sometimes etched in a 10 % citric acid, followed by coating with gold or carbon films. Microstructural features including the microcracks were observed on a scanning electron microscope (SEM).

3. Results and discussion

Fig. 1 shows a SEM micrograph of a cross-section of the RHA50 composite. Although the temperature for the hot isostatic pressing was as low as 825 ^{o}C, dense hydroxyapatite matrix was achieved. However, under this low temperature, microcracks were found in the dense HA matrix and the microcracks were often located around the 316L fibres. Fig. 2 shows a SEM micrograph of a cross-section of the CHA50 composite. The large number of pores present suggested that the calcined HA powder could not be densified under the 825 ^{o}C HIPing condition. This was due to the reduced sinterability of the calcined HA powder. The problem was that microcracks were also observed in the porous HA matrix. The microcracks were again around the 316L fibres.

Fig. 3 shows a SEM micrograph of a cross-section of the CHA50H composite. The HA matrix formed from the calcined HA powder was fully densified under 875 ^{o}C, which was just 50 ^{o}C higher than the temperature used for the CHA50 composite. However, microcracks were still found in the dense HA matrix and near the 316L fibres. Careful examination revealed that the interface was not a sharp one but one with a layer thickness. It can be imagined that the surfaces of the 316L fibres were oxidised due to inter-diffusion of elements across the boundaries. The interfacial layer was likely to be a mixture or a solid solution of HA and Cr_2O_3 based phases.

Fig. 4 and Fig. 5 show SEM micrographs of cross-sections of the CHA50GZ composite. The matrix was actually a dense composite of HA and Y-TZP. The addition of Y-TZP into HA was to increase the fracture strength of the matrix. However, microcracks were still observed. Thus a stress responsible for the microcracks was still higher than the fracture strength of the composite matrix.

Fig. 6 shows a SEM micrograph of a cross-section of the CHA50GS composite. The 316L fibres were preferentially rather than randomly distributed, which was due to the uniaxial loading condition of the SPS process. The cross-section of the CHA50GS composite was polished and etched with a 10% citric acid. Thus microcracks could be seen clearly in contrast to those

microcracks feebly visible on a polished surface. Thus, in spite of the short time used in the SPS process, which resulted in a mild degree of microcracking, microcracks were still unavoidable in the HA-316L composite system.

From Fig. 1 to Fig. 5, especially Fig. 3, one can notice the presence of the dark and elongated areas. One possible reason for the occurrence of the said microstructural feature could be the precipitation of chromium carbides along the stainless steel grain boundaries. The stainless steel 316L used was supposed to have a low carbon content. However, it was likely that the 316L fibres were subjected to an increase of carbon content through diffusion (carburizing). The origin of the carbon could be the graphite foils used, which could result in either solid free carbon or carbon containing vapours in the matrices of the composites. The increased carbon content at least near the 316L fibre surfaces, coupled with the relatively slow cooling rate of 10 ^{o}C/min., tended to result in the precipitation of chromium carbides, resulting in the local depletion of chromium content and the reduction of corrosion resistance. In other words, after implantation, the 316L stainless steel would undergo severe intergranular corrosion by physiological fluids and therefore limit its medical applications. A possible solution without changing to other metal fibres such as titanium alloy would be the use of boron nitride powder or foil for the diffusion barrier between the specimens and the capsules (cans). The starting powders should also be of a low carbon content. Fast cooling rate could reduce the extent of carbide precipitation, but may also cause the problem of thermal shock of the ceramic-based composites.

So far it has been demonstrated that microcracks are popular in the HA-316L composite system. It is important to understand the origin of the microcracks. The microcracks were not formed due to the polishing process, as polishing scratches have different appearance. The microcracks were also not likely to result from the differential sintering shrinkage of different regions, because a pressure was used at a high temperature to achieve full densification. The possible origin of the microcracks is believed to be the thermal residual stresses built up during the cooling process. The thermal residual stresses were due to the difference in thermal expansion coefficient between the 316L fibres and the HA matrices. Since the microcracks were predominantly found around and near the 316L fibres, one can isolate a fibre with a layer of HA matrix from the rest of the composite. This isolated element can then be used to calculate the thermal residual stresses using a two-cylinder model [10]. However, a cross-section of the two-cylinder model is used for simplicity to estimate the thermal residual stress in this paper.

Fig. 7 shows the model of a normal cross-section of the 316L fibre with a layer of HA matrix. The nature of the stresses (i.e. tensile or compressive) in the radial and the tangential directions in the 316L fibre and the HA layer can be imagined. Since the thermal expansion coefficient of 316L is 19.6 x 10^{-6} $^{o}C^{-1}$ [11], and that of HA is 16.9 x 10^{-6} $^{o}C^{-1}$ [12], one can imagine that during cooling, the 319L fibre tends to pull the HA layer towards the centre of the cross-section. Thus the 316L fibre tends to exert a tensile stress, σ, in the radial direction in the HA layer, which can be estimated using

$$\sigma = E\Delta\alpha\Delta T \qquad (1)$$

where $\Delta\alpha$ = (19.6-16.9) x 10^{-6} $^{o}C^{-1}$, ΔT = 800 ^{o}C (for example), E = 100 GPa (the Young's modulus of HA) [13].
Thus, σ = 216 MPa is obtained. This value is surprisingly high compared to the fracture strengths of the hot pressed or hot isostatic pressed HA ceramics, which were around 100 MPa [4]. Thus, it is possible that the microcracks were caused by the thermal residual stress. The round shaped microcracks near the 316L fibres also indicated the tensile stress in the radial direction that caused the microcracks propagating in the tangential direction.

The understanding of the origin of the microcracks could lead to some possible solutions to the microcracking problem. According to equation 1, if the temperature for densification can be

decreased, the thermal stresses can also be decreased. One simple way would be the use of a glass second phase in the hydroxyapatite matrices. The glass phase will act as a sintering aid and improve the strength of the matrices. The glass phase has another advantage, i.e, above a certain temperature (e.g., so-called anneal point), the glass still creeps, and stress can be relieved through the conversion of elastic strain to plastic strain. Another possibility is the introduction of leucite as a second phase, which is known to be biocompatible and have much higher thermal expansion coefficient than that of hydroxyapatite, making it possible to closely match the thermal expansion coefficient of the stainless steel fibres. One could also make use of an interlayer between the fibres and the matrices, which can smoothen the physical property change across the interface. However, such an interlayer is expected to be difficult to realise with the current thin and short fibres. In this regard, continuous 316L fibres or thin 316L foils would be more suitable for the application of the interlayer [14].

4. Conclusions

Hydroxyapatite-316L fibre composites were prepared under various conditions. Both internal factors such as composition and external factors such as densification temperature and pressure were considered. Full densification could be achieved and an interfacial layer was formed due to inter-diffusion of elements at high temperatures between the 316L fibres and the hydroxyapatite matrices. However, microcracks were commonly observed in the hydroxyapatite matrices and predominantly near the 316L fibres. Such microcracks were originated from a thermal residual stress due to the difference in thermal expansion coefficient of the 316L fibres and the hydroxyapatite matrices. The effects of the microcracks on the fracture strength and the fracture toughness of the composites need to be investigated additionally.

Acknowledgments

This paper has been in mind for a few years. Some results were obtained in Australia and some in Singapore. Thus, the people to be acknowledged are numerous, including A.J. Ruys and B.K. Milthorpe in the University of New South Wales and K.A. Khor and H.B. Guo in the Nanyang Technological University.

References

[1] F.B. Bagambisa, J. Ulrich, W. Schilli, J. Biomed. Mater. Res. 27 (1993) 1047.
[2] R.R. Rao, H.N. Roopo, T.S. Khannan, J. Mater. Sci: Mater. Med. 8 (1997) 511.
[3] M.A. Lopes, F.J. Monteiro, J.D. Santos, Biomaterials 20[21] (1999) 2085.
[4] W. Suchanek, M. Yoshimura, J. Mater. Res. 13[1] (1998) 94.
[5] J. Li, H. Liao, L. Hermansson, Biomaterials 12[18] (1996) 1787.
[6] A. Socarczyk, M. Klisch, M. Blazewicz, J. Piekarczyk, L. Stobierski, A. Rapacz-Kmita, J. Euro. Ceram. Soc. 20 (2000) 1397.
[7] G. De With, A. J. Corhijn, J. Mater. Sci. 24[9] (1998) 3411.
[8] T. Murakami, A. Kitahara, Y. Koga, M. Kawahara, H. Inui, M. Yamaguchi, Mater. Sci. Eng. A 239-240 (1997) 239.
[9] S. Yoo, J.R. Groza, T.S. Sudarshan, K. Yamazaki, Scripta Materialia 34[9] (1996) 1383.
[10] W. Lawrence, G.A.D. Briggs, C.B. Scruby, and J.R.R. Davies, J. Mater. Sci. 28 (1993) 3635.
[11] N.A. Waterman and M.F. Ashby, Elsevier Materials Selector (Elsevier Applied Science, London, 1991) p. 914.
[12] J.-W. Choi, Y.-M. Kong, H.-E. Kim, J. Am. Ceram. Soc. 81[7] (1998) 1743.
[13] M. Knepper, S. Moricca, and B.K. Milthorpe, Biomaterials 18 (1997) 1523.

[14] D. C. Clupper, J. J. Mecholsky, Jr., G. P. Latorre, and D. C. Greenspan, J. Mater. Sci. Lett. 20 (2001) 959.

Figure captions

Fig. 1 SEM micrograph showing the microcracks in the dense HA matrix (dark) and near the 316L fibre (bright) (sample: RHA50).

Fig. 2 SEM micrograph showing the microcrack in the porous HA matrix (dark) and near the 316L fibre (bright) (sample: CHA50).

Fig. 3 SEM micrograph showing the microcracks in the dense HA matrix (dark) and near the 316L fibre (bright with cavities) (sample: CHA50H).

Fig. 4 SEM micrograph showing the microcrack in the HA + 15 vol% Y-TZP composite matrix (Y-TZP bright; HA dark) and near the 316L fibre (bright) (sample: CHA50GZ).

Fig. 5 SEM micrograph showing the microcracks in the HA + 15 vol% Y-TZP composite matrix (Y-TZP bright; HA dark) and near the 316L fibre (bright) (sample: CHA50GZ).

Fig. 6 SEM micrograph showing the microcracks in the HA matrix (grey) and near the 316L fibres (dark) (sample: CHA50GS; etched and gold coated).

Fig. 7 A schematic diagram showing a cross-section of the two concentric cylinder model.

Table 1
Specimens prepared under various conditions

Sample	Matrix	316L fiber, 20 vol%	Processing	Pressure, MPa	Temperature, ^{o}C	Time, min.
RHA50	Raw HA	50 μm	HIP	140	825	180
CHA50	Calcined HA	50 μm	HIP	140	825	180
CHA50H	Calcined HA	50 μm	HIP	140	875	180
CHA50GZ	Calcined HA + 15 vol% Y-TZP	50 μm	HIP	140	950	90
CHA50GS	Calcined HA	50 μm	SPS	20	950	10

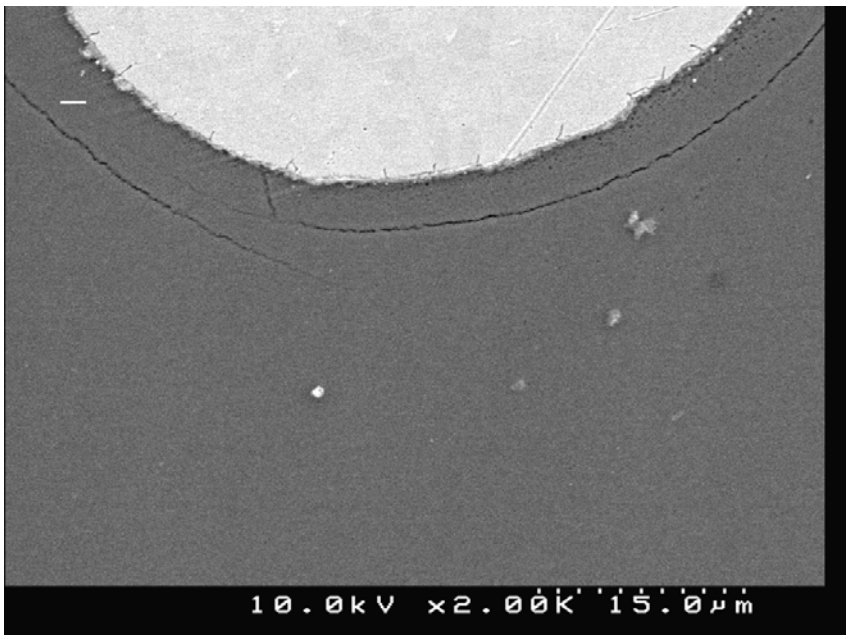

Fig. 1

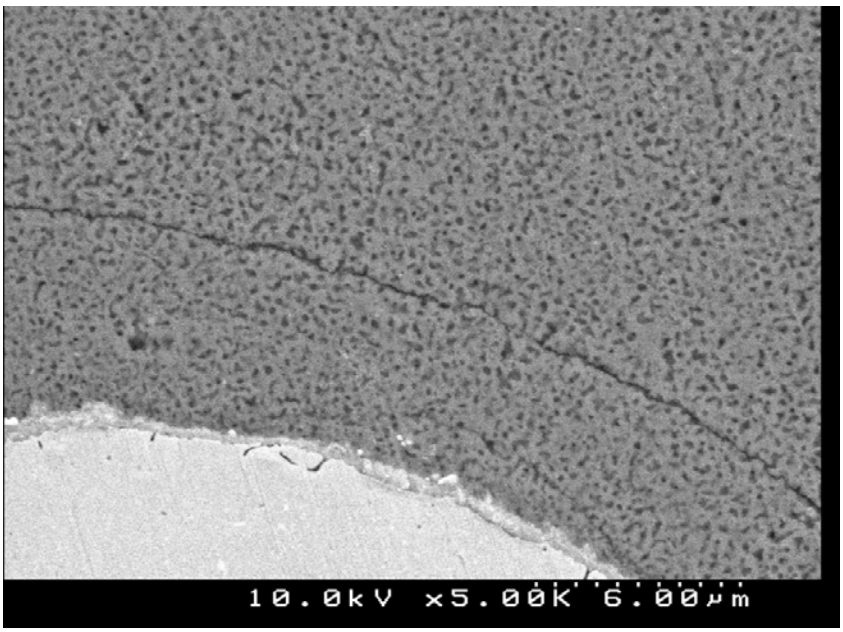

Fig. 2

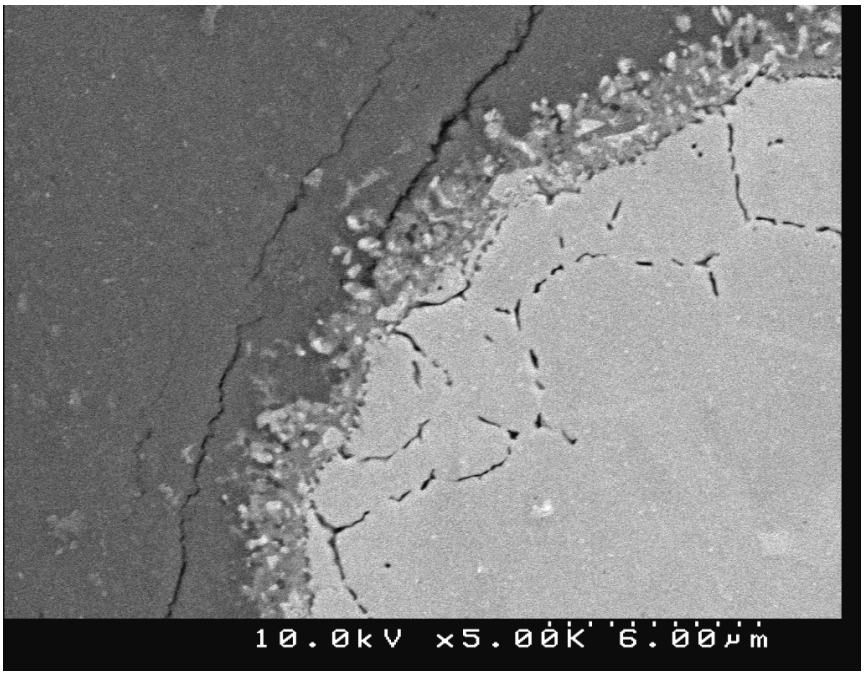

Fig. 3

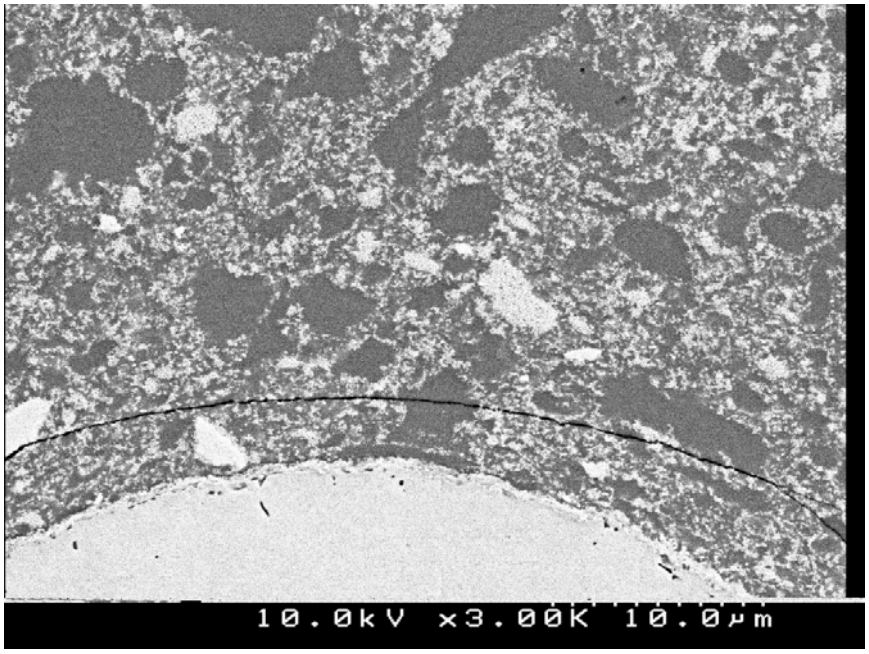

Fig. 4

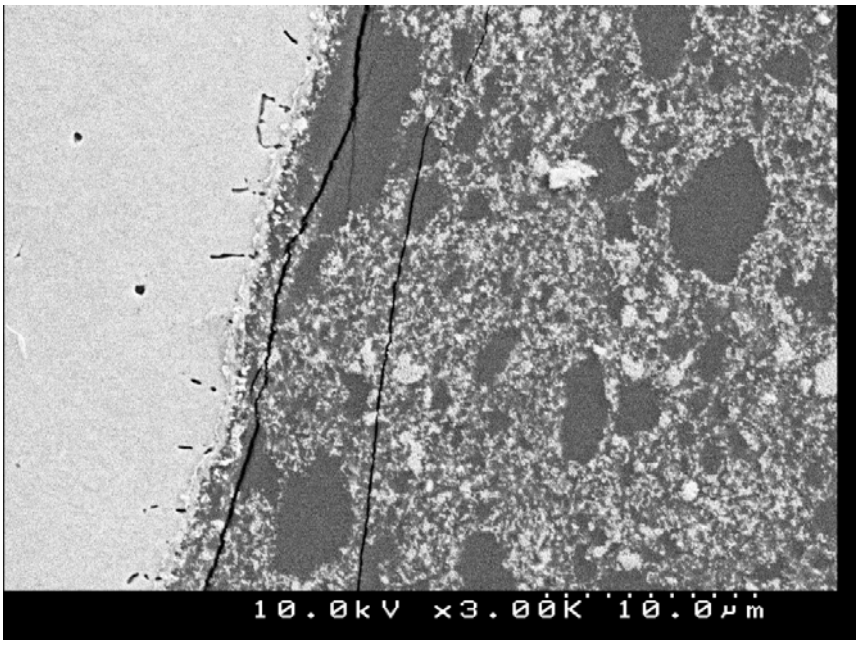

Fig. 5

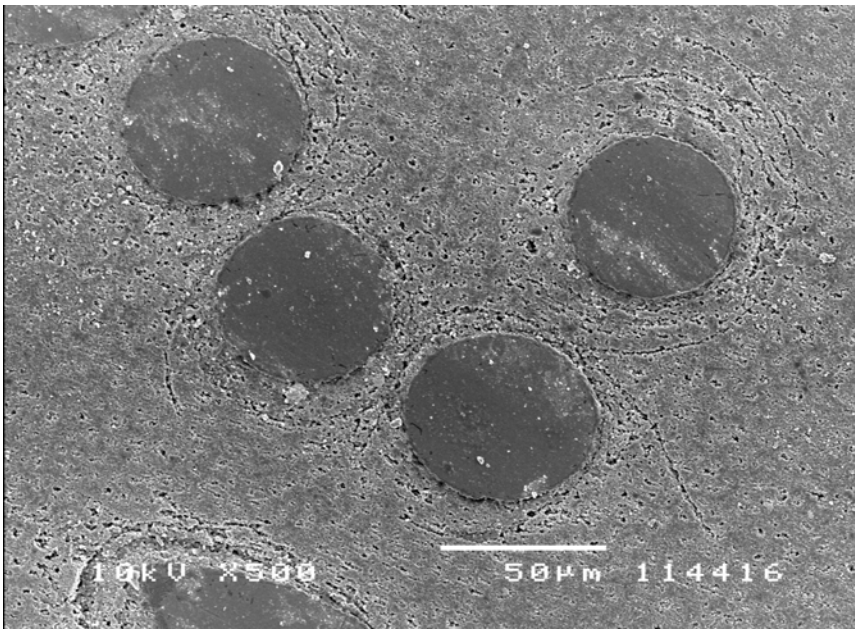
10kV X500
50µm 114416

Fig. 6

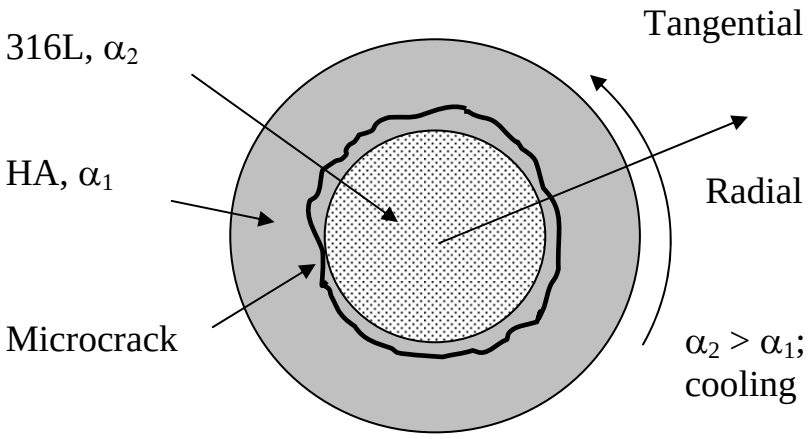
316L, α_2
HA, α_1
Microcrack
Tangential
Radial
$\alpha_2 > \alpha_1$; cooling

Fig. 7